



Transurethanization reaction as an alternative for melt modification of polyamide 6

Lucas Dall Agnol¹ · Hérlon Luiz Ceratti¹ · Diana Favero¹ · Silvana Pereira Rempel¹ · Licia da Silva Alves Schiavo¹ · Juliano Roberto Erzen^{1,2} · Fernanda Trindade Gonzalez Dias¹ · Otávio Bianchi¹

Received: 12 February 2019 / Accepted: 10 April 2019
© The Polymer Society, Taipei 2019

Abstract

This work presents an interesting alternative for melt modification of polyamide 6 (PA6). Transurethanization was employed as an effective strategy for this purpose. At high temperatures (>160 °C), the dissociation of urethane groups and subsequent reaction with PA6 end groups result in chain grown. The effect of TPU incorporation (2–10 wt.%) into PA6 on the microstructure, rheology, and thermal and mechanical performance of PA6/TPU blends was investigated. The chemical reactions between PA6 and TPU were elucidated using a model reaction of amino acid and MDI. The phase morphology of the blends did not show defined phases of TPU. However, it was noticed the formation of micrometric pores. Both the melting temperature and crystallinity of neat PA6 decreased with TPU incorporation. The production of a copolymer by terminal group reactions hinders the crystallization of polyamide with the reduction of nucleation and crystal growth. The increase in molar mass of PA6 can be confirmed by rheological measurements, in which an abrupt increase in viscosity was noted, as well as in the storage modulus. The impact strength of the blends significantly increased with the addition of TPU, whereas a discrete decrease occurred for the elastic modulus and tensile strength.

Keywords Polyamide 6/thermoplastic polyurethane blend · Transurethanization · Reactive extrusion · Intermeshing co-rotating twin-screw extrusion · Kinetics of crystallization

Introduction

Polyamide 6 (PA6) is a thermoplastic polymer extensively used in the manufacture of automobile parts, engineering products, and textile fibers because of its high mechanical and impact strength and good processability [1]. However, the marked use of these materials has resulted in post-consumer waste, increasing the demand for recycling, both for economic or environmental reasons [2]. During repeated processing of PA6, the polymer molecules are readily subjected to thermal, oxidative, and mechanical degradations,

promoting deterioration in the chemical structure of the polymer and, thus, restricting its final application [2, 3]. An interesting method of slowing down or avoiding the thermo-mechanical degradation occurring in PA6 melting reactive operations is the addition of small amounts of thermoplastic polyurethane elastomer (TPU) during reprocessing stages [4]. Molten polymer modification reactions may target specific molecular weight control to meet some particular engineering requirements [5]. PA6 and TPU can be blended since they have a high degree of structural similarity and specific intermolecular hydrogen interactions between amide and urethane groups [4, 6, 7]. TPU can be repeatedly melted and processed due to the absence of the chemical networks that usually exist in rubber. Unfortunately, there are only limited studies associated with PA6/TPU blends, which leaves a knowledge gap for obtaining thermoplastic elastomers materials with a favorable balance between processability and performance [8].

The PA6/TPU blends reported so far showed good compatibility, increased toughness and impact resistance, and reduced phase separation [7, 9–12]. The incorporation of 10 wt.% TPU in PA6 resulted in a gain of approximately 4 kJ.m⁻² in the

✉ Lucas Dall Agnol
ldagnol3@ucs.br

✉ Otávio Bianchi
otavio.bianchi@gmail.com

¹ Postgraduate Program in Materials Science and Engineering (PGMAT), University of Caxias do sul (UCS), Caxias do Sul, RS, Brazil

² Mantoflex Indústria de Plásticos Ltda, Caxias do Sul, Brazil

impact resistance of the blend, with practically no change in the elastic modulus [11]. GunaSingh et al. [10] observed that the IZOD impact resistance of PA6 increased by 40% with the incorporation of 15 wt.% TPU. The addition of increasing amounts of TPU to PA6 also caused a decrease in both its melting and crystallization temperatures [12]. These changes are related to the blending effect on the crystal growth rate and the degree of crystallinity as a result of modifications in the nucleation process [12]. A reversion of the TPU polymerization reaction occurs during its melt processing due to the chemical equilibrium of the urethane group, which can dissociate and re-associate simultaneously around 150–200 °C, when its thermo-mechanical degradation begins. The dissociation of the urethane group results in the formation of free isocyanate (–NCO) and alcohol groups, a phenomenon known as transurethanization [13, 14]. It is evident that the TPU chain degradation rate depends on processing conditions such as time, temperature, shear rate, and residence time [15]. Under mild processing conditions (temperatures below 250 °C), equilibrium is quickly established between urethane linkages and free isocyanate and hydroxyl end groups [16].

Once PA6 and TPU are in the molten state, the amine (–NH₂) and carboxylic acid (–COOH) end groups of polyamide are more nucleophilic than the hydroxyl groups of TPU, so the –NCO group formed by dissociation can react and form amine and urea groups. The rate of urea formation is about 1000 times faster relative to the primary hydroxyl [13], thus increasing the molecular weight and the molecular weight distribution of PA6. Therefore, the dissociation of the urethane group during the reactive processing of PA6/TPU blends represents an interesting strategy of modifying PA6 melting properties by copolymerization at the interfacial region. Transurethanization technology can then be an alternative to the high recycle yield of nylon.

In this work, we are interested in evaluating the effects of the addition of fixed amounts of TPU (2–10 wt.%) into a PA6 matrix, relative to the chemical structure, morphology, crystallinity, rheology, and thermal and mechanical performance of the resulting blends. More than that, we also intend to show that the transurethanization reaction is a feasible approach for polyamide chemical modification, especially when thermo-mechanical degradation deteriorates PA6 properties.

Materials and methods

Materials and methods preparation

PA6, trade name UBE NYLON 61022B, was supplied by UBE Corporation Europe (Spain), with a density of 1.14 g/cm³ (DIN 53479:1976), a relative viscosity (96% H₂SO₄) of 3.37 (JIS K6810–94) and a melting point of 220 °C (ISO 11357-16). PA6's molar mass is 20,000 g/mol, and its

viscosity is 200 mL/g according to the manufacturer. Aromatic polyether-based thermoplastic polyurethane (TPU), trade name 980A, was supplied by Mantoflex Indústria de Plásticos Ltda (Brazil). The TPU has a density of 1.15 g/cm³ (ASTM D792–13), and a Shore A hardness of 80 (ASTM D2240–15).

4,4'-diphenylmethane diisocyanate (MDI), trade name Isonate 125 M, was purchased from Dow Chemical Company (Brazil), and the L-alanine (C₃H₇NO₂, molar mass = 89.09 g/mol) was supplied by Sigma Aldrich (USA). All solvents were analytical grade, and all other chemicals were used as received.

Reactive processing

The neat materials and PA6/TPU blends containing 2–10 wt% TPU were melt processed in an interpenetrating co-rotating twin-screw extruder with a 48 L/D and 16 mm diameter (D) (LTE 16–48, LabTech Engineering Company). The reactive extrusion was conducted with a 135 rpm screen speed (n) and a 225–280 °C temperature profile. The average residence time of the material in the extruder was 250 s. Before melt blending, the PA6 and TPU pellets were dried at 100 °C in a vacuum oven for 12 h to avoid hydration of the material. The materials were manually homogenized and fed into the extruder at a feed rate of 3 kg/h. A specific screw profile was developed for this study, combining transport and kneading elements (30, 45, and 90°) (Fig. 1).

After reactive extrusion, the samples were dried for 4 h at 80 °C and injection molded (9.8 MPa, 250 °C, 6 s and injection mold temperature of 80 °C) into shaped test specimens according to ASTM D-638, type IV for mechanical experiments. The same conditions were used to produce specimens for X-ray diffraction (XRD), Fourier transform infrared spectroscopy in attenuated total reflectance mode (ATR-FTIR), and small-amplitude oscillatory shear measurements (SAOS) analysis.

Structural analysis and blends morphology

The ATR-FTIR measurements were performed in a Perkin Elmer Impact 400 spectrometer from 4000 to 400 cm⁻¹, with 32 scans and 4 cm⁻¹ resolution (diamond crystal at 45°).

The morphology of the blends was investigated by field emission gun scanning electron microscopy (FEG-SEM) in a Tescan Mira 3 (Czech Republic) microscope. Small samples (30 mm × 3 mm × 1 mm) from the central core of the injection-molded bars were cryo-fractured by liquid nitrogen and immersed in dimethylformamide (DMF) for 24 h at 80 °C to extract the TPU phase and reveal the phase boundaries. All samples were sputter coated with gold before imaging.

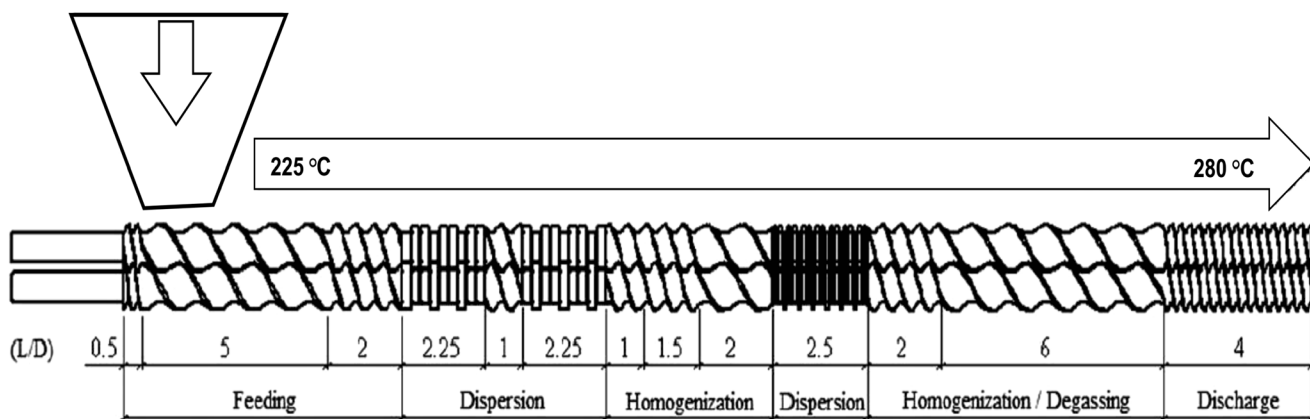


Fig. 1 Screw profile developed for the reactive extrusion

Crystalline microstructure and non-isothermal crystallization kinetics

The melting and crystallization behaviors and polymorphism of PA6 and its blends were investigated through differential scanning calorimetry (DSC) and X-ray diffraction (XRD). DSC analyses were performed in a Shimadzu DSC-60 under a nitrogen atmosphere with a 50 mL/min flow rate. The samples (~10 mg) were sealed in aluminum crucibles, heated at 10 °C/min to 280 °C, and kept at this temperature for 5 min to eliminate their thermal history. Then, the samples were cooled to ambient temperature at constant rates of 5, 10, 15, and 20 °C/min. The DSC data were used for calculation of the non-isothermal crystallization kinetics. To determine the melting behaviors, the samples were reheated to 280 °C at the same constant rates (5, 10, 15, and 20 °C/min).

The average crystallinity index (X_{cA}) was determined using Eq. 1 [17]:

$$X_{cA} = \frac{\Delta H_m}{\Delta H_m^0 \cdot \phi_{PA6}} \cdot 100 \quad (1)$$

where ϕ_{PA6} is the weight fraction of PA6 in the blends, ΔH_m is the fusion enthalpy of the samples (J/g) obtained by DSC measurements, and ΔH_m^0 is the fusion enthalpy of a 100% crystalline PA6 (190.9 J/g) [18]. The X_{cA} index was computed considering the average enthalpy at 5, 10, 15 and 20 °C/min heating rates.

XRD measurements were performed using a Shimadzu XRD-6000 diffractometer, operating in reflection mode using Cu $K_{\alpha 1}$ radiation ($\lambda = 1.540 \text{ \AA}$). Data were collected over 2θ angles ranging from 5 to 50° at a scanning rate of 0.5 °/min.

Reaction degree

The reaction degree was evaluated by selective solvent extraction. The solubility parameters of TPU [$11.68 \text{ (cal/cm}^3)^{1/2}$] and PA6 [$9.93 \text{ (cal/cm}^3)^{1/2}$] used in this work were

approximated from Fedors' molar volume [19]. The TPU phase was dissolved in DMF, which was selected for its similar solubility [$12.1 \text{ (cal/cm}^3)^{1/2}$] to TPU. The samples were placed in a 120-mesh sieve containing approximately 0.3 g of polymer and washed in a round-bottomed flask containing DMF at $150 \pm 3 \text{ °C}$ for 24 h. After solvent extraction, all samples were dried at 80 °C for 24 h. The reaction degree was determined by the weight difference between the extracted TPU and the one initially incorporated into the blend.

Small-amplitude oscillatory shear measurements (SAOS)

The rheological behavior of the neat polymers and their blends were studied in an Anton Paar MCR 301 rheometer with cone-plate geometry (25 mm and 1°). Sample discs (25 mm diameter and 3 mm thickness) were prepared by injection molding. The experiments were carried out under linear viscoelastic (300 Pa) conditions at 250 °C and a frequency range of 0.1–100 rad/s in a nitrogen atmosphere. For pure TPU, the measurement was performed at 230 °C.

Physico-mechanical properties

Tensile strength tests were conducted on an Emic DL2000 Universal Testing Machine according to ASTM D638–14. The crosshead speed was 50 mm/min. Five specimens from each sample were assayed. The Impact resistance tests were performed according to ASTM D256–10 using Type A specimens using a Ceast Resil 25 impact test equipment with a 1 J hammer. During all mechanical tests, the room temperature was maintained at $23 \pm 2 \text{ °C}$ and the relative humidity at $36 \pm 2\%$.

For the water uptake determination, three samples of each blend were initially dried at 100 °C for 48 h in a circulating air oven, thus obtaining the dry weight of the samples (W_s). The samples were then exposed to the environment, and their mass gain was monitored for 33 days, allowing the determination of the wet weight

of the materials (W_u). The water uptake (WU) was calculated using Eq. 2 [5]:

$$WU = \frac{W_u - W_s}{W_s} \cdot 100\% \quad (2)$$

The density of the samples was measured following ASTM standard D792–13.

Results and discussion

Reaction and phase morphology

The FTIR spectra of neat PA6 and TPU, and PA6/TPU 10 wt.% blend are presented in Fig. 2(a). The characteristic absorption bands of PA6 were clearly evidenced: 3293 cm^{-1} and 3082 cm^{-1} (NH); 1632 cm^{-1} (C=O); 1536 cm^{-1} (C-N); 2928 cm^{-1} and 2856 cm^{-1} (CH_2); 931 cm^{-1} (CO-NH); and 1461 cm^{-1} and 1415 cm^{-1} ($-\text{CH}_2-$ linked to NH and CO) [20]. The absorptions at 686 cm^{-1} and 1203 cm^{-1} are related to the α crystalline phase, whereas the bands at 1169 cm^{-1} are associated to γ and amorphous phases, indicating the coexistence of pseudohexagonal and monoclinic phases in the PA6 microstructure [20, 21]. Considering the TPU spectrum, absorptions due to the urethane group appeared at: 3302 cm^{-1} and 1528 cm^{-1} (NH); 1597 cm^{-1} , 818 cm^{-1} and 770 cm^{-1} (C=C in the presence of aromatic components); 1220 cm^{-1} and 1077 cm^{-1} (C-O and COO); 1203 cm^{-1} (C-OH); and 2918 and 2849 cm^{-1} (CH), 1414 cm^{-1} (CH_2). The presence of bands at 1731 cm^{-1} and 1701 cm^{-1} (C=O) with the concomitant absence of the absorption at 3460 cm^{-1} (free -NH) denotes a large number of hydrogen bonds in the sample [22, 23].

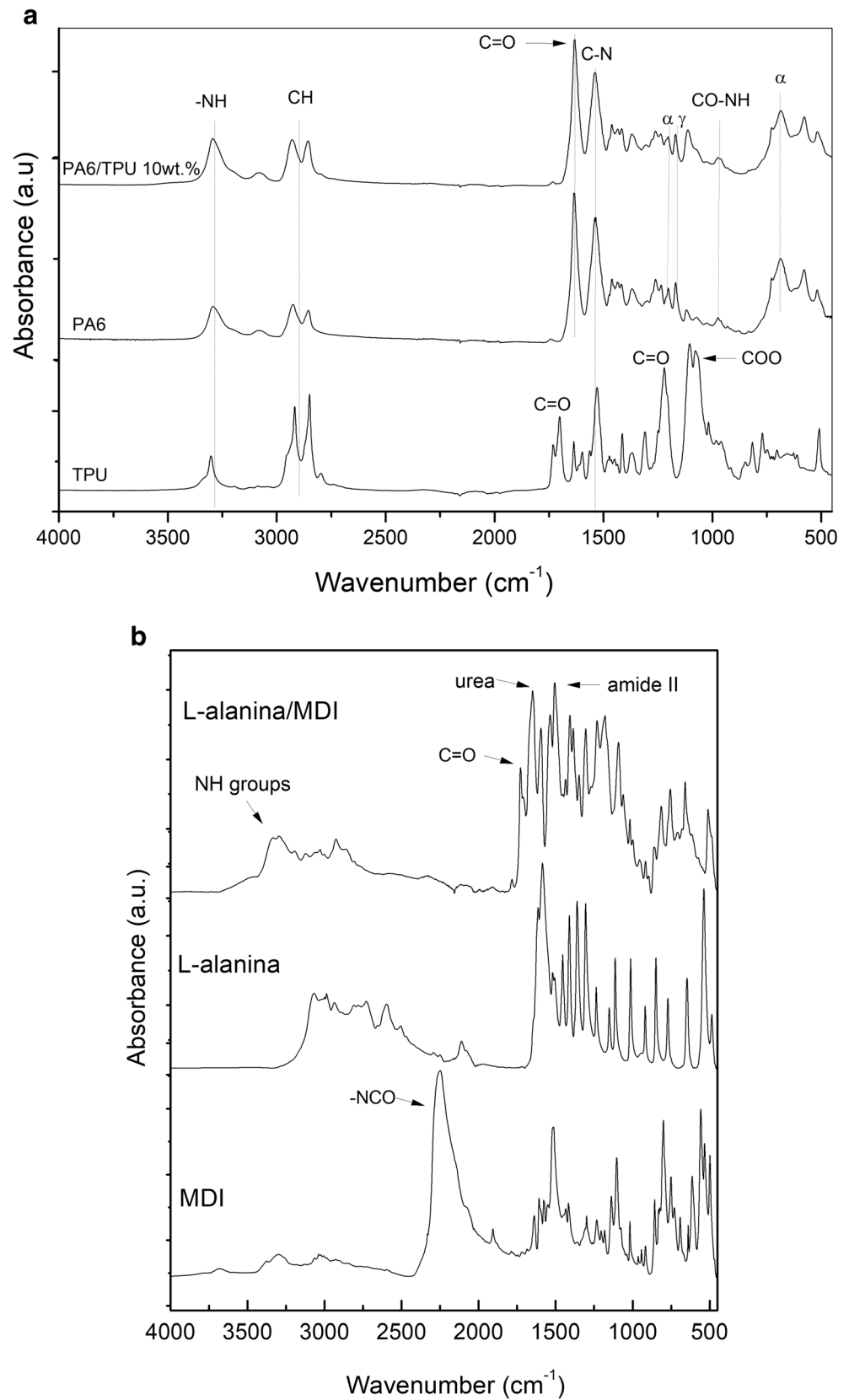
No significant differences were observed between the spectra of neat PA6 and PA6/TPU 10 wt.% blend, indicating that the absorptions of pure polymers overlapped the reaction traces between PA6 and the dissociated end chain of TPU. The only events observed in these spectra were an increase in the peak intensity at 3375 cm^{-1} and the presence of a small shoulder at 3433 cm^{-1} attributed to the stretching of hydrogen-bonded and free -NH groups [24]. According to the literature [24, 25], chemical reactions between -NCO, -NH₂ and -COOH functional groups can form urea and amide. The reactions between isocyanates and primary amines are very fast with a low activation energy, usually several kilocalories per mol, whereas the half-life of the reaction between aliphatic amines and aromatic isocyanates is in the order of milliseconds [25]. In addition to the stable carboamide binding to the acid end group of PA6, a secondary association between the -NH groups of PA6 and the -NCO groups was assumed, which can be further disassociated by the subsequent reaction with an amine to form urea [16, 25].

Due to the low molar fraction of functional groups formed relative to the main chain size, we proposed to study the associations between -NCO, -NH₂ and -COOH groups through a model reaction of a small amino acid with MDI. Thus, a higher relative amount of functional groups formed will contribute to a better understanding of the reaction between polyamide and polyurethane. The FTIR spectra of the components and the model reaction are shown in Fig. 2(b). The chemical reactions between PA6 and -R-NCO were studied by Franke and coworkers [25]. The ester group of the isocyanate compound appears as a shoulder in the amide I band, which suggests the presence of TPU in the blends. Also, the appearance of the characteristic peak of the -NH groups (3405 cm^{-1}) indicates the formation of urea and amide groups. When the isocyanate group reacts with the carboxyl group, amide I absorption bands of the amide linkage appear in the 1595–1700 cm^{-1} region. The new band at 1614–1629 cm^{-1} was assigned to urea. Moreover, the absorptions at 1734 cm^{-1} and 1718 cm^{-1} can be attributed to free and hydrogen-bonded urethane carbonyl groups [4]. The amide II band relative to the urethane linkage also appeared at 1525 cm^{-1} [26]. The disappearance of the -NCO characteristic peaks (2268 cm^{-1}) was also evident, suggesting that isocyanate reacted with L-alanine. Therefore, this approach proved feasible in elucidating the reactions that occur between PA6 and TPU during melt processing. The reaction scheme is presented in Fig. 3.

Figure 4 shows the FEG-SEM micrographs of the fractured surfaces of PA6/TPU blends. All images exhibited spherically shaped pores (from 500 to 2500 nm diameter) regardless of the composition of the mixtures. The presence of pores can be explained by the reaction between carbamic acid and the urea group with the release of carbon dioxide (CO_2) [8]. For the non-etched samples, the images revealed significant relief differences with similar sizes. The addition of more significant amounts of TPU decreased the cracks and favored more smooth fractured regions, suggesting a compatible structure between PA6 and TPU through their polar groups. A similar phase morphology pattern was observed by Rätzsch et al. (1990), who attributed it to the presence of TPU phase in the blends [11]. Nevertheless, it was not possible to identify well-defined interfaces between PA6 and TPU phases.

It is well known that isocyanate is highly reactive toward many functional groups. Under some circumstances, it can even self-react by dimerization, trimerization, linear polymerization, and condensation with elimination of carbon dioxide to form uretidinone, isocyanurate, poly-1-nylon, and carbodiimide or a secondary bond (allophanate), respectively. However, the first three products can hardly exist at 200 °C, a temperature that promotes the cleavage of the urethane linkage and the formation of carbodiimide. The carbodiimide or allophanate is still reactive toward active-hydrogen-containing compounds, thus generating branched or

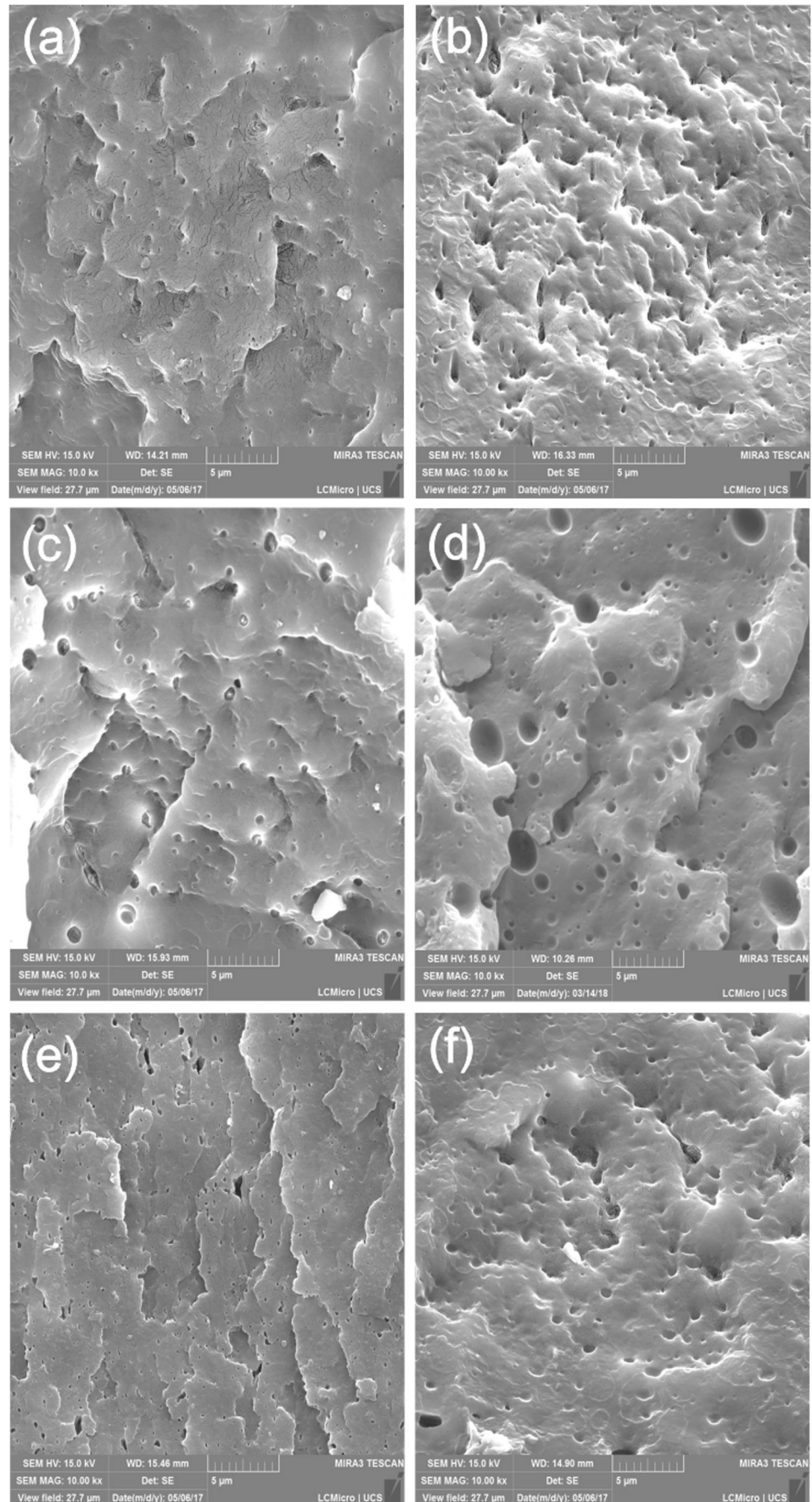
Fig. 2 (a) ATR-FTIR spectra of neat TPU and PA6, and PA6/TPU 10 wt.% blend (b) ATR-FTIR spectra of MDI, L-alanina, and the reaction between L-alanina/MDI



crosslinked structures [16]. Therefore, the possibility of forming gelled compositions during processing was also

investigated. The blends were dissolved in formic acid to verify the gel formation by chain crosslinking [5]. As

Fig. 4 Phase morphologies of PA6/TPU blends of different compositions **(a)** 2 wt.% TPU, **(b)** 2 wt.% TPU extracted, **(c)** 5 wt.% TPU, **(d)** 5 wt.% TPU extracted, **(e)** 10 wt.% TPU e **(f)** 10 wt.% TPU extracted



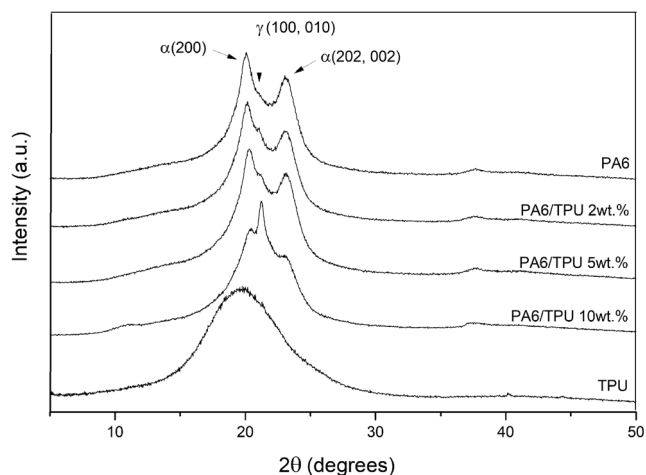


Fig. 5 X-ray diffractograms for neat PA6, TPU, and PA6/TPU blends

intermolecular hydrogen bonds of the PA6 chains, preventing the orderly arrangement to produce α -phase crystals. The addition of TPU to PA6 destroys its crystallinity to some extent.

Changes in the crystalline structure of the PA6 caused by the presence of TPU in the blends were observed not only through XRD but also in the DSC measurements. Figure 6 shows typical DSC curves relative to the first cooling and the second heating cycles (10 °C/min) for neat PA6, and PA6/TPU blends containing different amounts of TPU. Neat TPU did not show a distinct melting peak or crystallization.

Neat PA6 crystallizes at about 177 °C and melts around 220 °C with a shoulder relative to the γ -phase melting at 214 °C [31, 32]. A decrease in melting temperature in comparison to neat PA6 was observed for the PA6/TPU blends. The reaction between PA6 and TPU reduces the molecular motility of the PA6 chains, making it difficult for PA6 to form crystals, which require a lower temperature to melt due to its less perfect lamellar structures [12]. The decreasing trend in the melting temperature of the blends is attributed to the diluent effect of the soft segment on the crystallizable PA6, mainly by hydrogen interactions between the urethane groups in TPU and the amide groups of PA6. The crystallization curve of the sample containing 10 wt.% TPU showed a peak near 120 °C associated with the PA6/TPU copolymer formed at the interfacial region. The PA6/TPU copolymer formed has a lower crystallization temperature than neat PA6. Thus, the higher the number of reactive groups ($-\text{NH}_2$ and $-\text{COOH}$) the higher the amount of PA6/TPU copolymer at the interface.

Table 1 summarizes the DSC data for neat PA6 and its blends with TPU. The enthalpy and crystallinity values are lower for the blends as compared to the neat PA6, confirming that the presence of TPU destroys the primary crystallinity of PA6 [7, 12]. The incorporation of TPU into the blends also contributed to the formation of γ -phase crystals, as shown by the XRD results. The γ -phase crystals are less stable (metastable) than α -phase crystals and can be converted into α -phase by annealing, which causes the formation of

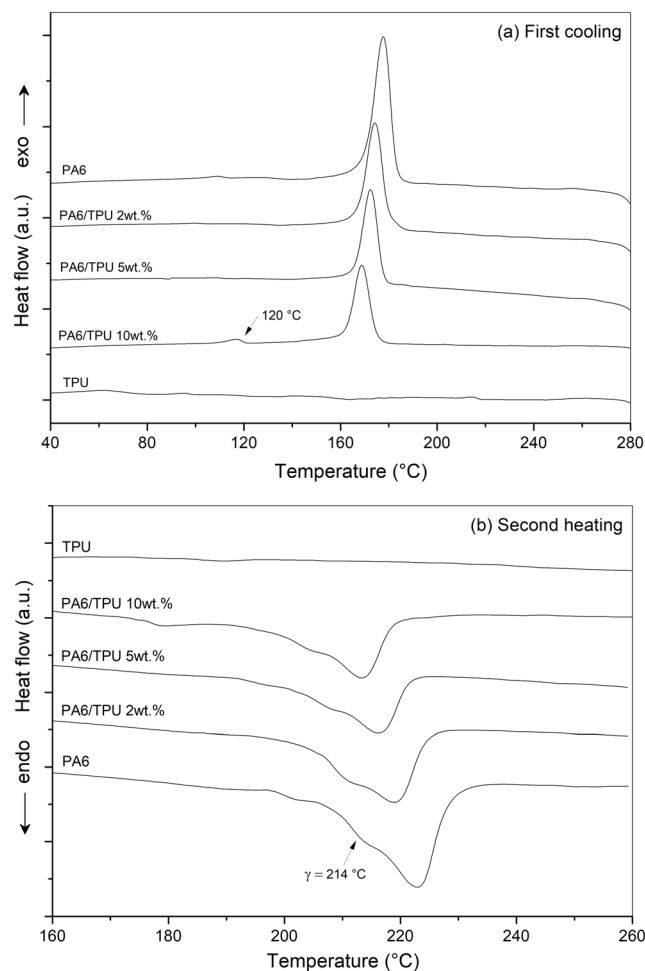


Fig. 6 DSC curves for neat PA6, TPU, and PA6/TPU blends during (a) the first cooling and (b) second heating cycle at a constant rate of 10 °C/min

hydrogen bonds between the adjacent parallel chains [30]. The decrease in enthalpy values, crystallinity index, and melt temperatures are related to the creation of PA6/TPU copolymer at the chain end region. This results in a restriction in the lamellar fold, producing a considerable amount of amorphous polyamide.

From the DSC results, it is evident that the reaction between PA6 and TPU causes a reduction in crystallinity, and consequently, in the crystallization rate of polyamide. The non-isothermal experimental data were analyzed regarding the degree of supercooling (ΔT_C) [33]. ΔT_C is defined as the temperature difference between melting in the heating scan and the onset of crystallization in the cooling scan and can act as a guide for ranking the polymers on a scale of crystallization rates. The variation of ΔT_C with cooling rate can be fitted to a linear Equation [33]:

$$\Delta T_C = (P\varphi) + \Delta T_C^0 \quad (3)$$

where the intercept, ΔT_C^0 , is related to the inherent crystallizability of the polymer and is the degree of

Table 1 DSC data of neat PA6 and PA6/TPU blends taken at different cooling/heating rates

Sample	First cooling			Second heating				R*
	φ (°C/min)	T _c (°C)	ΔH_c (J/g)	T _m (°C)	ΔH_m (J/g)	X _{CA} (%)	P (min ⁻¹)	
PA6	5	185.3	46.3	211.8; 220.4	39.3	18.8	0.824	26.1
	10	181.1	45.2	211.7; 220.5	34.1			
	15	177.8	44.5	211.5; 221.9	36.4			
	20	173.6	46.3	211.2; 222.6	33.7			
PA6/TPU 2 wt.%	5	181.3	34.5	210.8; 219.1	29.4	14.9	0.802	29.2
	10	176.2	34.6	210.4; 220.3	25.9			
	15	172.5	36.8	209.7; 220.4	27.8			
	20	169.9	38.6	209.7; 220.8	28.7			
PA6/TPU 5 wt.%	5	180.7	37.6	210.3; 217.6	31.3	16.3	0.796	27.7
	10	174.8	41.1	209.3; 217.5	30.4			
	15	172.2	38.3	209.8; 218.8	28.3			
	20	166.6	39.2	208.4; 219.9	28.1			
PA6/TPU 10 wt.%	5	171.9	38.9	202.9; 212.9	28.7	15.2	0.534	31.3
	10	172.6	37.1	204.3; 214.4	27.6			
	15	170.5	31.6	204.8; 216.6	24.1			
	20	169.2	32.8	206.3; 217.9	23.9			

PA6: polyamide 6; TPU: thermoplastic polyurethane; φ : heating rate; T_c: crystallization temperature; ΔH_c : crystallization enthalpy; ΔH_m : apparent enthalpy of fusion per gram of blend; X_{CA}: crystallinity index; P: process sensitivity factor; R*: correlation coefficient

supercooling required in the limit of zero cooling rate, and P is a process sensitivity factor that accounts for the kinetic effects. The variation of the degree of under-cooling with cooling rate indicates the ability of polymer molecules to respond to thermal changes.

The value of P indicates the sensitivity of the polymer structure to the reactive processing conditions. Thus, the lower P values for PA6/TPU blends indicate a low sensitivity of these materials to variations in the cooling rates. Changes in P and ΔT_C^0 values manifest the effect of molecular weight increases. In thermodynamic terms, this means that the entropy ($\Delta S_m = \Delta H_m/T_m$) of the molten state is increasing because of the greater difficulty of PA6 chains to organize.

Since the reactive processing of PA6 with TPU modifies the rate of phase transformation, the energetic barriers for the crystallization of PA6 and PA6/TPU mixtures could be determined from the activation energy ($\Delta E_{a(X_T)}$), which also considers the barrier energies for nucleation and growth. The temperature dependence of a non-isothermal crystallization does not follow Arrhenius behavior, so in this study, the concept of the effective activation energy associated with a particular relative crystallinity degree ($\Delta E_{a(X_T)}$) was employed. The parameter ($\Delta E_{a(X_T)}$) was calculated through the differential isoconversional method proposed by Friedman (FR) (Eq. 4) [34]:

$$\ln\left(\frac{dX_T}{dt}\right)_{(X_T),i} = C - \frac{\Delta E_{a(X_T)}}{RT_{(X_T),i}} \quad (4)$$

where parameter C is the natural logarithm of the pre-exponential factor (A) multiplied by a function that describes the crystallization model, dX_T/dt is the instantaneous crystallization rate, R is the universal gas constant, and T is the absolute temperature.

The relative degree of crystallinity, X_T , was calculated using Eq. 5, where dH_c/dT is the crystallization enthalpy at an infinitesimal temperature, and T_0 and T_∞ are, respectively, the onset and end crystallization temperatures.

$$X_T = \frac{\int_{T_0}^T \left(\frac{dH_c}{dT}\right) \cdot dT}{\int_{T_0}^{T_\infty} \left(\frac{dH_c}{dT}\right) \cdot dT} \quad (5)$$

By selecting an appropriate relative degree of crystallinity, the values of $(dX_T/dt)_{(X_T),i}$ were correlated to the corresponding crystallization temperature, $T_{(X_T),i}$, for each heating rate applied.

According to Eq. 3, the effective activation energy at a given relative degree of crystallinity, $\Delta E_{a(X_T)}$, is obtained from the slope ($\Delta E_a/R$) of the linear fitting of $\ln\left(\frac{dX_T}{dt}\right)_{(X_T),i}$ versus $1/T_{(X_T),i}$. The kinetic results presented in Fig. 7 show the dependence of $\Delta E_{a(X_T)}$ as a function of the relative crystallization degree for neat PA6 and PA6/TPU blends. The

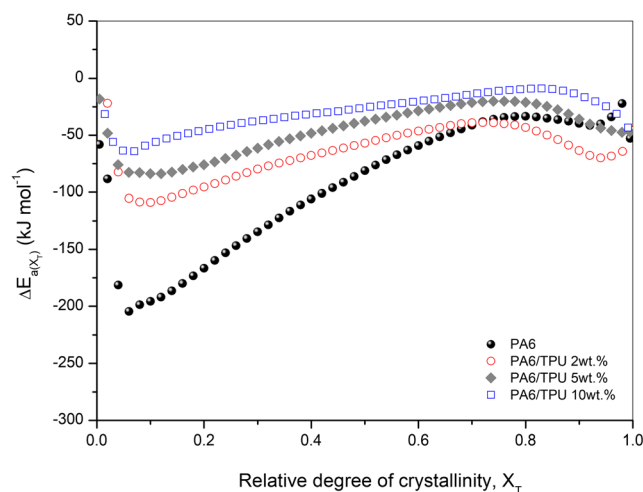


Fig. 7 Activation energy as a function of the relative crystallization degree for PA6 and PA6/TPU blends

activation energies computed were negative and increased with increasing amount of TPU in the blends. The increasing tendency of $\Delta E_{a(X_T)}$ for the blends indicates that polymer crystallization is disadvantaged as the crystallization progresses. The PA6 chains are restricted in mobility to crystallize during solidification due to the increase in molecular weight [31, 35].

The macroscopic crystallization rate of polymers can be determined by the rates of nucleation process and nuclei growth, which can be estimated by Eqs. (6) and (7) [36, 37].

$$r = r_0 e^{\left(\frac{-E_D - \Delta F^*}{k_B T}\right)} \quad (6)$$

$$\Delta F^* \sim \frac{1}{(\Delta T_C^0)^2} \quad (7)$$

where r is the crystallization rate, r_0 is the pre-exponential factor, k_B is the Boltzmann constant, E_D is the activation energy for diffusion of molecules or chain segments across the phase boundary, T_m is the melting point, and ΔF^* is the maximum free energy required for nucleus formation, which is inversely proportional to the degree of the supercooling (ΔT_C^0). According to Eq. (7), the nucleation process plays a decisive role in the overall crystallization rate at the beginning of the non-isothermal crystallization, and the number of crystal nuclei increases rapidly. In this case, the term $1/(\Delta T_C^0)^2$ is relatively large, because T is close to the melting temperature, T_m , corresponding to the highest ΔF^* value [36]. Consequently, $\Delta E_{a(X_T)}$ is initially fairly negative ($\Delta E_{a(0.1)} < -197$ kJ/mol for neat PA6) and increases with decreasing T , a typical anti-Arrhenius behavior. Thus, the increment in $\Delta E_{a(X_T)}$ occasioned by the increase of ΔT_C^0 values results in a dramatic reduction of ΔF^* and an increase in the E_D contribution of the crystallization rate promoted by the reactive terminal groups (-NCO, -COOH and -NH₂).

The Hoffman-Lauritzen theory about surface nucleation is often applied to the analysis of the spherulitic growth rate for the melt crystallization of polymers. This approach is generally adopted from direct polarized light microscopy (PLM) data or indirect isothermal DSC measurements. Nonetheless, using PLM to probe the growth rate of crystals may suffer interference from the different crystal spherulites and the precise control over crystallization temperature. For isothermal DSC measurements, the baseline used for the determination of the time to half-time crystallization is difficult to identify, which limits the calculation of the growth rate of crystals [38, 39].

Vyazaovkin and Sbirrazzuoly [38] developed a method to obtain the Hoffman-Lauritzen parameters from non-isothermal $\Delta E_{a(X_T)}$ data (Eq. 8):

$$\Delta E_{a(X_T)} = U^* \frac{T^2}{(T - T_\infty)^2} + K_g R \frac{(T_m^0)^2 - T^2 - T_m^0 T}{(T_m^0 - T)^2 T} \quad (8)$$

where T is the average temperature associated with a given relative degree of crystallinity, T_∞ is a hypothetical temperature at which polymer chain diffusion stops (usually, T_∞ is 30 K below the glass transition temperature, T_g), T_m^0 is the equilibrium melting temperature of the polymer, U^* is the activation energy for polymer chain diffusion across the melt/crystal interface, K_g is a nucleation parameter proportional to the surface free energy required for the formation of the nuclei of critical size, and R is the universal gas constant. Hoffman-Lauritzen parameters (U^* and K_g) were computed using the nonlinear least-squares Levenberge-Marquardt algorithm (LMA) [40, 41]. The T_m^0 and T_∞ values adopted for the PA6 were 501 K and 313 K, respectively [30, 42].

Figure 8 shows the activation energy fitted data as a function of the mean temperature associated with a specific relative crystallization degree for PA6 and its blends containing TPU. PA6 shows two crystallization regimes and an inflection

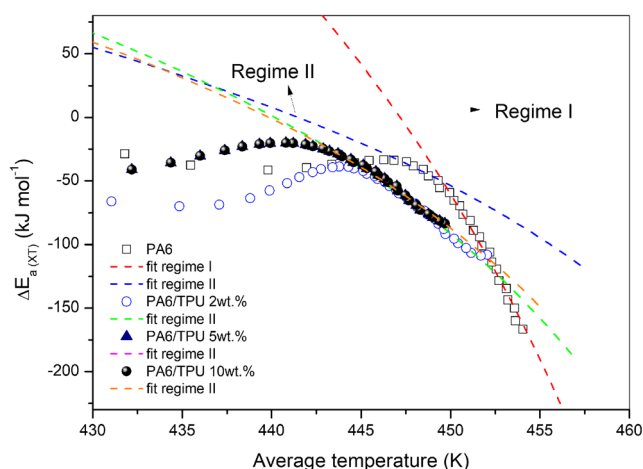


Fig. 8 Determination of the Hoffman-Lauritzen parameters from the activation energy variation with the mean temperature, using Eq. (8)

point at 449 K, while the blends present only one crystallization regime. According to Hoffman-Lauritzen’s theory [43], the constant K_g is associated with three regimes. For regimes I and III, its theoretical value is 4, whereas for regime II it is 2. In regime I, the nucleation rate is slow, and thus one molecular chain can crystallize at a time. In contrast, the nucleation rate of regimen II is faster than the crystallization rate of each macromolecule, so multiple surface nuclei occur on the same crystallization surface. Regime III is associated with a fast crystallization rate, and consequently, only a few folds of a chain occur before reentering the amorphous phase, which is usually related to a very large supercooling. The Hoffman-Lauritzen parameters are summarized in Table 2.

The K_g and U^* values decreased with increasing amount of TPU in the blends. Regime I was not observed for PA6/TPU mixtures, probably because of the small interface existing between the phases, which increases the nucleation rate. The increase of molar mass, in contrast, retards the growth of the crystalline phase. Therefore, the decrease in K_g values could indicate an increase in the entropy of the chain folding, and hence the formation of a less uniform folding surface [44]. The reduction of K_g values (~ 1) was also attributed to the increased flexibility of the chain [45]. In our context, the TPU used is a polyether, and this could act directly in reducing the hydrogen bonds density.

Rheology and physicomechanical properties

Figure 9 shows the storage and loss moduli as a function of angular frequency for neat PA6, TPU, and PA6/TPU blends. For all samples, a pseudo-liquid viscous behavior, in which the loss modulus (G'') was higher than the storage modulus (G'), could be observed. Also, the storage modulus of the blends increased in comparison with neat polymers, probably due to a synergistic effect between the PA6 terminals and the dissociated TPU products. However, the initial values of the elastic plateau for blends containing 5 and 10 wt.%

Table 2 Hoffman-Lauritzen parameters for neat PA6, and PA6/TPU blends

Sample	Regime	K_g ($10^{-5} K^2$)	U^* ($kJ mol^{-1}$)	R^2
PA6	I	3.38	33.7	0.984
	II	1.16	8.51	0.922
PA6/TPU 2 wt. %	I	—	—	—
	II	1.80	12.5	0.9992
PA6/TPU 5 wt. %	I	—	—	—
	II	1.67	11.4	0.987
PA6/TPU 10 wt. %	I	—	—	—
	II	1.08	7.17	0.994

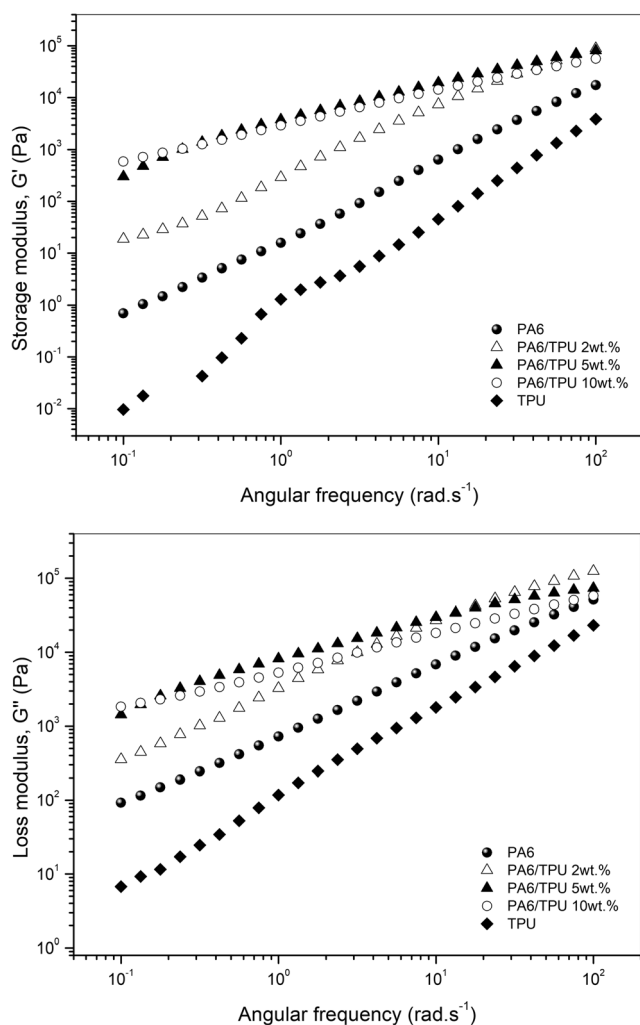


Fig. 9 Storage modulus (G') and Loss modulus (G'') versus angular frequency curves for pure PA6, TPU, and PA6/TPU blends

TPU were similar. The viscoelastic behavior of PA6/TPU blends depends on the number of terminal groups in PA6 chains. The values of G' and G'' vary proportionally to the molar masses of the blends, confirming the values obtained for the reaction degrees.

Polymeric chains that are flexible and fully relaxed exhibit a power law behavior, with scaling properties of approximately $G' \sim \omega^2$ and $G'' \sim \omega^1$ (where ω is the angular frequency) [46]. However, practically all materials show some deviation from the flexible chains (see Table 3). The smallest deviation is noted for the neat polymers. The increase in molar mass caused by the reactions between PA6 and TPU accentuates the deviation from the flexible chains. Thus, it is believed that the higher the deviation, the more polydisperse the material becomes [47].

The complex viscosity (η^*) profiles of the materials were fitted using the Cross model (Eq. (9)) [47] by means the nonlinear least-squares Levenberg–Marquardt algorithm (LMA) [48]. The correlation coefficients were >0.99 , and the results are presented in Table 3.

Table 3 G' and G'' slopes vs. angular frequency and Cross rheological constants for the PA6, TPU, and PA6/TPU blends

Sample	Slope of G' vs. ω	Slope of G'' vs. ω	η_0^* (Pa.s)	λ (s)	m	r^2
PA6	1.34	0.83	749.1	0.001	0.549	0.963
PA6/TPU 2 wt. %	0.79	0.90	3353.8	0.013	0.846	0.972
PA6/TPU 5 wt. %	1.05	0.96	20,482.7	1.335	0.618	0.991
PA6/TPU 10 wt. %	0.66	0.39	3.8×10^{10}	1.8×10^{14}	0.477	0.996
TPU	1.66	1.04	—	—	—	—

PA6: polyamide 6; TPU: thermoplastic polyurethane; G' : storage modulus; G'' : loss modulus; ω : angular frequency. η_0^* : complex viscosity at zero frequency; λ : constant; $m \rightarrow 1$ = pseudoplastic behavior, $m \rightarrow 0$ = Newtonian fluid behavior; r^2 : correlation coefficient

The Cox–Merz relation was used to convert the dynamic data in steady-flow viscosities.

$$\eta(\dot{\gamma}) = \frac{\eta_0}{1 + (\lambda \cdot \dot{\gamma})^m} \quad (9)$$

$$\eta(\dot{\gamma}) \Big|_{\dot{\gamma} \rightarrow 0} = \eta^*(\omega) \Big|_{\omega \rightarrow 0} \quad (10)$$

where η is the shear-dependent viscosity, η_0 the zero-shear viscosity, $\dot{\gamma}$ represents the shear rate, ω is the angular frequency, λ is a time-dependent parameter associated with Newtonian plateau transition, and $m = 1 - n$ (where n is the power-law index, a dimensionless parameter that accounts for shear thinning).

Neat PA6 shows Newtonian plateau regions at low frequencies. However, the reaction of PA6 with TPU results in reducing the Newtonian plateau region, contributing to the transition from the Newtonian to the non-Newtonian regime. The transition from the Newtonian regime to the pseudoplastic regime occurs because at lower frequencies the shear rate does not affect the convoluted form of the chains. At higher frequencies, the polymeric chains begin to orient towards the flow, causing the viscosity to decrease rapidly [49]. A high value of λ implies a relatively large shear-dependent contribution to structural breakdown under shear. When λ is large, breakdown occurs at relatively low shear rates (frequencies). Therefore, the transition from the Newtonian plateau occurs at lower frequencies for the blends in comparison with neat PA6. This trend is attributed to the increased viscous dissipation resulting from the presence of the interface formed during the melt reaction between PA6 and TPU phases [50]. Parameter η_0^* increases proportionally with the amount of TPU in the blends and provides a direct indication that the increase in molar mass is occurring.

The results of the mechanical tests are shown in Table 4. The elastic modulus data for neat TPU were not presented due to the non-linear elastic behavior was observed.

Table 4 Physico-mechanical properties of neat PA6 and TPU and PA6/TPU blends

Sample	Elastic modulus (MPa)	Maximum Tensile strength (MPa)	Strain at break (%)	Tenacity (J)	Impact resistance (kJ.m ⁻²)	Density (kg.m ³)	H ₂ O absorption (33 days)/%
PA6	2528 ± 228	80 ± 2	127 ± 42	32 ± 23	7.5 ± 2.5	1.122 ± 0.001	13.3 ± 0.6
PA6/TPU 2 wt.%	2240 ± 255	73 ± 4	447 ± 23	250 ± 11	16.8 ± 3.4	1.117 ± 0.003	13.5 ± 0.7
PA6/TPU 5 wt.%	2559 ± 67	76 ± 3	363 ± 96	200 ± 56	22.6 ± 1.4	1.114 ± 0.003	13.4 ± 0.4
PA6/TPU 10 wt.%	2211 ± 119	68 ± 1	281 ± 60	197 ± 28	24.9 ± 3.2	1.111 ± 0.002	14.2 ± 0.7
TPU	–	9.2 ± 1.2	657 ± 24	–	49.1 ± 3.9	1.098 ± 0.003	3.9 ± 0.2

PA6: polyamide 6; TPU: thermoplastic polyurethane

A discrete reduction of the elastic modulus and tensile strength were observed for the blends containing 2 wt.% and 10 wt.% TPU, in comparison with neat PA6. The opposite effect was observed for tenacity, which reached a maximum value of 250 ± 11 J for the mixture with 2 wt.% TPU, an increase of 681.2% over neat PA6. As the TPU is an elastomer with low tensile stress compared to PA6, its addition to the crystal structure of polyamide destroys the crystalline regions, as shown by the DSC and XRD results for the PA6/TPU blends. The hydrogen bonds formed between PA6 and TPU contribute to the reduction of phase separation, and thus, the polymeric blend shows higher strain at break values when compared to neat PA6. Similar mechanical results were reported in the literature [28]. The reduction of the elastic modulus of the blends is directly associated with the TPU addition, which by presenting mechanical properties inferior to PA6, causes the reduction of crystallinity [7]. The elastic modulus of the blend containing 10 wt.% TPU had a reduction of approximately 13% in comparison to neat PA6, behavior that was also observed by GunaSingh et al. [10] for PA6/TPU blends with 15 wt.% TPU.

The addition of TPU improved the impact strength of the blends in comparison with neat PA6, reaching the maximum value of 24 kJ/mm² for a 10 wt.% TPU content in the mixture. The use of an elastomeric phase in polyamides represents a strategy for an impact modifier, and it is often noted as having additive rule behavior [7]. The blends showed a nonlinear reduction in density values with increasing amounts of TPU, and this decrease does not follow the mixing rule (see Table 4). As observed in the micrographs, the decrease in density may be associated with the increase in the number of pores generated during the reaction. As expected, the water absorption data showed that the water uptake for TPU was much lower when compared to PA6 samples. However, there was no significant difference between PA6 and PA6/TPU blends (see Table 4). The PA6 and PA6/TPU blends absorbed water until the 28th day of testing, after which the absorption tended to stabilize. The PA6 is part of a set of polymers that can absorb up to 10 wt.% by weight of water in the atmosphere [51]. For the PA6/TPU blends, pore formation and crystallinity reduction seem to play a critical role in the water uptake, since both contribute to the diffusion of water into the structure.

Conclusion

This work aimed at the melt modification of PA6, especially using the transurethanization reaction as a strategy for promoting the molar mass increase of PA6. A model reaction using amino acid and MDI, suggested the formation of amine and urea groups during the processing of PA6/TPU. The PA6/TPU copolymers disturbed to some extent the crystallization of PA6. Increasing TPU content caused a reduction in the melting temperature of the blends, probably because of the diluent effect of the soft segment on the crystallizable PA6. The increase in molar mass of PA6 also resulted in an increment of the storage modulus and the complex viscosity at zero frequency of the blends, providing a direct indication of the reaction between the PA6 terminals and the dissociated TPU product. The pores generated during the reaction, and detected in SEM micrographs, did not affect the mechanical performance. The impact strength of PA6 was significantly increased by the addition of TPU, accompanied by a decrease in tensile properties because of the crystallinity reduction of the blends. No significant differences in water absorption or density values were observed between PA6 and PA6/TPU blends. We also found that the reactive processing did not form secondary reaction products that could crosslink the polymeric chain. Therefore, the incorporation of small amounts of TPU can be a viable alternative to PA6 recycling by melt processing due to the increase of the molar mass promoted by the transurethanization reaction.

Acknowledgements The authors thank Conselho Nacional de Desenvolvimento Científico e Tecnológico (CNPq, Brazil) for financial support (Grant 308241/2015-0) and the Brazilian Agency *Coordenação de Aperfeiçoamento de Pessoal de Nível Superior - Brasil (CAPES)* - (Finance Code 001) for scholarships. The authors also thank Mantoflex Indústria de Plásticos Ltda for the donation of the polymers, Laboratório Central de Microscopia Prof. Israel Baumvol for the FEG-SEM analysis, and Carlos Romoaldo and Debora Guerra for help with mechanical testing.

Compliance with ethical standards

Conflict of interest The authors declare that they have no conflict of interest.

References

- Lozano-González MJ, Rodriguez-Hernandez MT, Gonzalez-De Los Santos EA, Villalpando-Olmos J (2000) Physical–mechanical properties and morphological study on nylon-6 recycling by injection molding. *J Appl Polym Sci* 76(6):851–858
- Li HB, Wu JW, Huang YQ, Runt J, Huang CM, Huang KS, Yeh JT (2018) Properties of polyamide 612/poly (vinyl alcohol) blends and their impact on free volume and oxygen barrier properties. *J Polym Res* 25(9):195
- Goitisoló I, Eguiazábal JI, Nazábal J (2008) Effects of reprocessing on the structure and properties of polyamide 6 nanocomposites. *Polym Degrad Stab* 93(10):1747–1752
- Hou LL, Liu HZ, Yang GS (2006) A novel approach to the preparation of thermoplastic polyurethane elastomer and polyamide 6 blends by in situ anionic ring-opening polymerization of ϵ -caprolactam. *Polym Int* 55(6):643–649
- Bondan F, Ernzen JR, Amalvy J, Machado AV, Martins JDN, Bianchi O (2016) Influence of dynamic crosslinking on the morphology, crystallization, and dynamic mechanical properties of PA6,12/EVA blends. *J Appl Polym Sci* 133(46):44206 (44212p)
- Hou L, Liu H, Yang G (2006) Preparation and characterization of thermoplastic polyurethane elastomer and polyamide 6 blends by in situ anionic ring-opening polymerization of ϵ -caprolactam. *Polym Eng Sci* 46(9):1196–1203
- Zhou S, Huang J, Zhang Q (2014) Mechanical and tribological properties of polyamide-based composites modified by thermoplastic polyurethane. *J Thermoplast Compos Mater* 27(1):18–34
- Yi C, Peng Z, Wang H, Li M, Wang C (2011) Synthesis and characteristics of thermoplastic elastomer based on polyamide-6. *Polym Int* 60(12):1728–1736
- Genovese A, Shanks RA (2001) Simulation of the specific interactions between polyamide-6 and a thermoplastic polyurethane. *Comput Theor Polymer Sci* 11(1):57–62
- GunaSingh C, Soundararajan S, Palanivelu K (2013) Studies on mechanical, thermal properties and characterization of nanocomposites of nylon-6–thermoplastics poly urethane rubber [TPUR] blend. *IOSR J Appl Chem* 4(1):65–75
- Rätzsch M, Haudel G, Pompe G, Meyer E (1990) Interaction between polymers. *J Macromol Sci A* 27(13–14):1631–1655
- Haponiuk J, Balas A (1995) Thermal properties of polyamide 6/polyurethane blends. *J Therm Anal Calorim* 43(1):211–214
- Hentschel T, Münstedt H (2001) Kinetics of the molar mass decrease in a polyurethane melt: a rheological study. *Polymer* 42(7):3195–3203
- Deepa P, Jayakannan M (2008) Solvent-free and nonisocyanate melt transurethane reaction for aliphatic polyurethanes and mechanistic aspects. *J Polym Sci A Polym Chem* 46(7):2445–2458
- Puau JP, Cassagnau P, Bozga G, Nagy I (2006) Modeling of polyurethane synthesis by reactive extrusion. *Chem Eng Process* 45(6):481–487
- Lu QW, Hoyer TR, Macosko CW (2002) Reactivity of common functional groups with urethanes: models for reactive compatibilization of thermoplastic polyurethane blends. *J Polym Sci A Polym Chem* 40(14):2310–2328
- Shi X, Zhang J, Jin J, Chen S (2008) Non-isothermal crystallization and melting of ethylene-vinyl acetate copolymers with different vinyl acetate contents. *Express Polym Lett* 2(9):623–629
- Chiang C-R, Chang F-C (1997) Polymer blends of polyamide-6 (PA6) and poly (phenylene oxide) (PPO) compatibilized by styrene-maleic anhydride (SMA) copolymer. *Polymer* 38(19):4807–4817
- Van Krevelen DW, Te Nijenhuis K (2009) Properties of polymers: their correlation with chemical structure; their numerical estimation and prediction from additive group contributions. Elsevier
- Wu Q, Liu X, Berglund LA (2002) FT-IR spectroscopic study of hydrogen bonding in PA6/clay nanocomposites. *Polymer* 43(8):2445–2449
- Kong W, Yang Y, Liu Z, Lei J (2017) Structure-property relations of novel polyamide-6 elastomers prepared through reactive processing. *J Polym Res* 24(10):168
- Lee BS, Chun BC, Chung Y-C, Sul KI, Cho JW (2001) Structure and thermomechanical properties of polyurethane block copolymers with shape memory effect. *Macromolecules* 34(18):6431–6437
- Seymour R, Estes G, Cooper SL (1970) Infrared studies of segmented polyurethane elastomers. I. Hydrogen bonding. *Macromolecules* 3(5):579–583
- Skrockienė V, Žukienė K, Jankauskaitė V, Baltušnikas A, Petraitiienė S (2016) Properties of mechanically recycled polycaprolactone-based thermoplastic polyurethane/polycaprolactone blends and their nanocomposites. *J Elastom Plast* 48(3):266–286
- Franke C, Pötschke P, Rätzsch M, Pompe G, Sahre K, Voigt D, Janke A (1993) Wirkung von Diisocyanat als reaktiver Koppler in TPU/PA6-Blends. *Angew Makromol Chem* 206(1):21–38
- Tuominen J, Kylvä J, Seppälä J (2002) Chain extending of lactic acid oligomers. 2. Increase of molecular weight with 1,6-hexamethylene diisocyanate and 2,2'-bis(2-oxazoline). *Polymer* 43(1):3–10
- Stephens JS, Chase DB, Rabolt JF (2004) Effect of the electrospinning process on polymer crystallization chain conformation in nylon-6 and nylon-12. *Macromolecules* 37(3):877–881
- Zo HJ, Joo SH, Kim T, Seo PS, Kim JH, Park JS (2014) Enhanced mechanical and thermal properties of carbon fiber composites with polyamide and thermoplastic polyurethane blends. *Fiber Polym* 15(5):1071–1077
- Njuguna J, Pielichowski K, Desai S (2008) Nanofiller-reinforced polymer nanocomposites. *Polym Adv Technol* 19(8):947–959
- Guo B, Zuo Q, Lei Y, Du M, Liu M, Jia D (2009) Crystallization behavior of polyamide 6/halloysite nanotubes nanocomposites. *Thermochim Acta* 484(1–2):48–56
- Liu Y, Yang G (2010) Non-isothermal crystallization kinetics of polyamide-6/graphite oxide nanocomposites. *Thermochim Acta* 500(1–2):13–20
- Haponiuk J (2000) Phase transitions of polyamide 6/polyurethane blends compatibilized by copolyurethaneamides. *J Therm Anal Calorim* 60(1):45–52
- Nadkarni VM, Bulakh NN, Jog JP (1993) Assessing polymer crystallizability from nonisothermal crystallization behavior. *Adv Polym Technol* 12(1):73–79
- Friedman HL (1964) Kinetics of thermal degradation of char-forming plastics from thermogravimetry. Application to a phenolic plastic. *J Polym Sci C: Polym Symp* 6(1):183–195
- Li W, Liu J, Zhang X, Zhao Y, Wang D (2012) Synergetic effect of polyamide 1212 and diisocyanate on performance improving of thermoplastic polyurethane via melt compounding. *J Appl Polym Sci* 125(2):1077–1083
- Vyazovkin S, Sbirrazzuoli N (2002) Isoconversional analysis of the nonisothermal crystallization of a polymer melt. *Macromol Rapid Commun* 23(13):766–770
- Vyazovkin S, Sbirrazzuoli N (2003) Isoconversional analysis of calorimetric data on nonisothermal crystallization of a polymer melt. *J Phys Chem B* 107(3):882–888
- Vyazovkin S, Sbirrazzuoli N (2004) Isoconversional approach to evaluating the Hoffman–Lauritzen parameters (U^* and K_g) from the overall rates of nonisothermal crystallization. *Macromol Rapid Commun* 25(6):733–738
- Chan TW, Isayev AI (1994) Quiescent polymer crystallization: modelling and measurements. *Polym Eng Sci* 34(6):461–471
- Marquardt DW (1963) An algorithm for least-squares estimation of nonlinear parameters. *J Soc Ind Appl Math* 11(2):431–441

41. Levenberg K (1944) A method for the solution of certain non-linear problems in least squares. *Q Appl Math* 2(2):164–168
42. Huang JW, Chang CC, Kang CC, Yeh MY (2008) Crystallization kinetics and nucleation parameters of nylon 6 and poly(ethylene-co-glycidyl methacrylate) blend. *Thermochim Acta* 468(1–2):66–74
43. Lauritzen Jr JI, Hoffman JD (1973) Extension of theory of growth of chain-folded polymer crystals to large undercoolings. *J Appl Phys* 44(10):4340–4352
44. Lonkar SP, Morlat-Therias S, Caperaa N, Leroux F, Gardette JL, Singh RP (2009) Preparation and nonisothermal crystallization behavior of polypropylene/layered double hydroxide nanocomposites. *Polymer* 50(6):1505–1515
45. Tsanaktsis V, Bikiaris DN, Guigo N, Exarhopoulos S, Papageorgiou DG, Sbirrazzuoli N, Papageorgiou GZ (2015) Synthesis, properties and thermal behavior of poly(decylene-2,5-furanoate): a biobased polyester from 2,5-furan dicarboxylic acid. *RSC Adv* 5(91):74592–74604
46. Ferreira CI, Bianchi O, Oviedo MAS, Oliveira RVBD, Mauler RS (2013) Morphological, viscoelastic and mechanical characterization of polypropylene/exfoliated graphite nanocomposites. *Polimeros* 23(4):456–461
47. Bianchi O, Júnior HLO, Canto LB, Mauler RS, de Oliveira RVB (2016) Viscoelastic properties of PS–POSS hybrid materials prepared by reactive processing. *Polym Test* 54:159–167
48. Cox W, Merz E (1959) Rheology of polymer melts – a correlation of dynamic and steady flow measurements. In: International symposium on plastics testing and standardization. ASTM International
49. Liu Y, Li S-C, Liu H (2013) Melt rheological properties of LLDPE/PP blends compatibilized by cross-linked LLDPE/PP blends (LLDPE-PP). *Polym Plast Technol Eng* 52(8):841–846
50. do Amaral FCN, Emzen JR, Fiorio R, Martins JDN, Dias FTG, Avolio R, Bianchi O (2018) Effect of the partially hydrolyzed EVA-h content on the morphology, rheology, and mechanical properties of PA12/EVA blends. *Polym Eng Sci* 58(3):335–344
51. Piao H, Kiryu Y, Chen L, Yamashita S, Ohsawa I, Takahashi J (2019) Influence of water absorption on the mechanical properties of discontinuous carbon fiber reinforced polyamide 6. *J Polym Res* 26(3):63

Publisher's note Springer Nature remains neutral with regard to jurisdictional claims in published maps and institutional affiliations.